Joint Measurement of Target Angle and Angular Velocity Using Interferometric Radar with FM Waveforms

Jason Merlo and Jeffrey A. Nanzer
Department of Electrical and Computer Engineering, Michigan State University
{merlojas, nanzer}@msu.edu

***Abstract*—An architecture for a direct-downconversion complex correlation interferometric radar capable of the direct, joint measurement of angle and angular velocity of a point-target is presented. Due to the simplicity of the system, this technique can be implemented on existing radars with distributed receivers and a transmitter capable of frequency modulation. Derivations for the interferometric measurement of angle and angular velocity and guidelines for the design of such a system are presented. Simulations are provided for the proposed system with varying pulse-width, antenna baseline, and pulse center frequency. The results for all simulations show a low root-mean-square error which demonstrates the feasibility of the proposed system.**

***Index Terms*—Correlation Interferometry, Angle Estimation, Angular Velocity Estimation, Distributed Array, Distributed Radar**

I. Introduction

In many radar applications, the objective is to determine the position and velocity vectors of a remote target. While many radars have been able to measure the radial distance and radial velocity since the early 20^{th} century, a particular interest has been placed on also determining the angle and angular velocity of a moving target relative to the receiver to create a fully constrained representation of the target state in multiple dimensions [1], [2]. Knowledge of the target state at a given time enables the use of a wide class of filtering, prediction, and smoothing algorithms to be used to estimate the target's past and present states as well as predict future states [3], [4]. Knowing this information is valuable in many domains such as airspace monitoring, space object tracking, automated driving, and human computer interfaces to name a few [5]–[8]. In addition to state tracking and prediction, it has also been shown that through observing the micro-Doppler signature of a target, a target's type and motion or activity can also be estimated [9], [10]. Measuring micro-motion tangential to the radar such as those of rotating blades or of a pedestrian's body movements tangential to the radar thus affords more accurate classification of uncooperative targets when not moving in the radial direction [11], [12].

Historically, measuring the angular, or cross range, velocity of a target has been accomplished using mechanically steered antennas or phased arrays. Both of these approaches involve scanning a transmit beam across the search space and measuring the angle of arrival of the reflection to estimate angle at which the target was located; from this angular rate may be derived by measuring the rate of change of the angle estimate over multiple successive samples. This can introduce error in angle and angle rate measurement based on scanning angle accuracy and target measurement angle accuracy; furthermore, due the the requirement to collect multiple samples, there will be an inherent delay in angular rate estimation. Recent developments have shown that these constraints can be alleviated by employing correlation interferometry which enables the angular velocity of a target anywhere in search-space to be observed instantaneously, without scanning, using only two receivers [11], [13]. More recently, it has been shown that absolute target angle can also be directly measured through the combined use of correlation interferometry and linear frequency modulation (LFM) [14].

In this paper, the simultaneous measurements of target angle and angular velocity using interferometric frequency modulated continuous-wave (FMCW) waveforms are presented. Due to the simplicity of the approach, this technique may be implemented on existing radar hardware which processes the signals received at an intermediate frequency (IF) or baseband digitally, without any hardware modification through the addition of a digital correlation process. While prior works have shown the efficacy of correlation interferometry to measure the absolute angle of a target at the carrier frequency [14], it will be further demonstrated that common heterodyne architectures are also well suited for measuring angle lending to the ability to implement this method on low-cost radars with low-IF or direct-downconversion front-end architectures and digital signal processing.

Section II will discuss the principle of operation of the interferometer as well as derive the method of measurement for both angle and angular velocity. In Section III design considerations for such a system will be discussed. Last, in Section IV a proposed architecture for an interferometric radar capable of jointly measuring the angle and angular velocity of a target will be presented followed by simulations of the proposed system to illustrate the operation of the device. Finally, the error between the estimate and ground-truth state for various system parameters will be presented. The simulations show a close agreement between the estimated and

978-1-7281-8942-0/20/$31.00 ©2020 IEEE

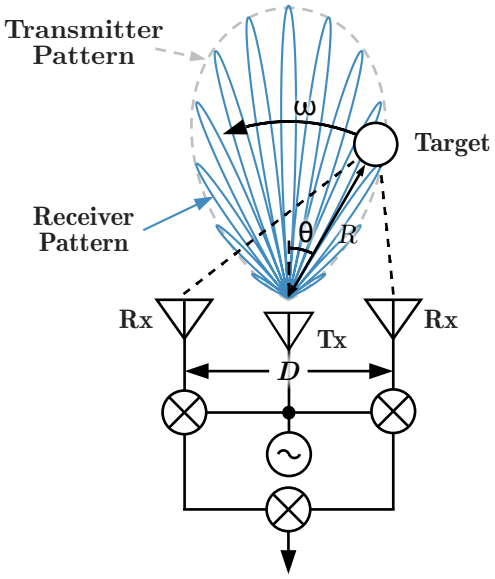

Fig. 1. An active correlation interferometer observing a point-target moving tangentially to the array. The fringe pattern formed by the summation of phases from the two receivers after correlation is shown in blue. All antennas have identical radiation patterns.

ground-truth state for measuring angle and angular velocity of a point object moving tangentially to the radar, demonstrating the feasibility of this architecture for such an application.

II. Target State Measurement Methods

The basic correlation interferometric radar, shown in Fig. 1, operates on the principle of measuring the frequency created by the interaction of an object moving angularly in space with the interference pattern of the receive antennas separated by a baseline D, which is typically multiple wavelengths for this application [13]. Generally, as the target interacts with the grating lobes, or fringe pattern, created by the distributed receive antenna elements, a frequency is induced at the correlator output which can be interpreted to determine the angular velocity of the target. However, with the addition of a modulated carrier waveform, the absolute angle of the target relative to the array is also able to be resolved [14].

To determine the angular velocity, the carrier frequency is typically held static over time as a simple, unmodulated continuous-wave (CW) waveform, which will hold constant the spatial frequency, and thus angular location, of the grating lobes produced by the receive antenna array. In this case, as the target moves past the broadside of the array, a frequency proportional to its angular velocity will be produced at the output of the correlator. To measure the absolute angle of the target relative to the array, the carrier can be swept over a range of frequencies which induces a change in the spatial frequency, and thus location, of the grating lobes in the receive antenna array. As this frequency is varied, the peaks and nulls of the grating lobes will be swept over the target generating a frequency response proportional to the angle of the target off broadside. In this technique, both of these effects are exploited simultaneously to determine the angle and angular velocity of the target, thus there will be two sources of modulation on the correlator output: the modulation caused by the angular motion of the object passing through the grating lobes, and the modulation caused by the chirp waveform sweeping the grating lobes across the object.

A. Signal Model

This analysis will focus on the LFM waveform due to its popularity in existing radar ranging systems, however, the transmitted waveform can, in theory, be any waveform used for measuring range in a typical radar system. In practice, practical limitations will require the waveform to be chosen to meet the requirements for angle and angular rate of the system. The analyses of angle and angular velocity estimation for pulsed LFM and FMCW waveforms are essentially identical; thus we will focus on a single LFM up-chirp for simplicity.

The transmitted LFM waveform can be described in terms of its desired angular frequency with respect to time,

$$\omega_s(t) = 2\pi\left(f_0 + \frac{\beta}{\tau}t\right);\ t \in [-\tau/2, \tau/2] \tag{1}$$

where f_0 is the center frequency, β is the total bandwidth, and τ is the length of the chirp (β/τ is also known as the chirp-rate) [1]. The transmitted waveform can be described as a complex exponential with the phase angle, found by integrating (1), as the argument,

$$s(t) = \exp\left[j\pi(2f_0 t + \frac{\beta}{\tau}t^2)\right]. \tag{2}$$

The signals measured at the receive antennas can be modeled as a time delayed copy of the original transmitted signal after being reflected off the target

$$r_c(t) = A\exp\left[j\pi(2f_0(t-\tau_d) + \frac{\beta}{\tau}(t-\tau_d)^2)\right] \tag{3}$$

where A is the received signal amplitude. The round-trip time of the signal is defined as $\tau_d = 2R/c$ where R is the distance from the antenna to the target surface and c is the speed of light in the medium. After down-conversion the signal will be

$$\begin{aligned} r(t) &= r_c(t)s^*(t) \\ &= A\exp\left\{j\pi\left[-2f_0\tau_d + \frac{\beta}{\tau}(\tau_d^2 - 2\tau_d t)\right]\right\}. \end{aligned} \tag{4}$$

By taking the time derivative of the phase $\phi(t)$ of this signal, the beat frequency can be obtained. Assuming a constant velocity model, $\frac{d}{dt}\tau_d = 2v_R/c$ where v_R is the radial component of the velocity of the target relative to the receive antenna. Thus, the beat frequency at the output of the mixer is

$$\begin{aligned} f_b(t) &= \frac{1}{2\pi}\frac{d\phi(t)}{dt} \\ &= \frac{1}{2}\frac{d}{dt}\left[-2f_0\tau_d + \frac{\beta}{\tau}\left(\tau_d^2 - 2\tau_d t\right)\right] \\ &= -\frac{2v_R}{\lambda} - \frac{2}{c}\frac{\beta}{\tau}\left(R + v_R t - \frac{4}{c^2}Rv_R\right) \end{aligned} \tag{5}$$

where λ is the wavelength of the transmitted signal. It can be seen that the range-Doppler coupling phenomenon is present; the first term is due to the Doppler shift and the second term is due to the range of the target. The familiar zero-Doppler case can be obtained by setting $v_R = 0$, resulting in $f_b(t) = -\frac{2}{c}\frac{\beta}{\tau}R$.

B. Cross Range Angular Velocity Measurement

It has been shown in [13], [15] that the angular velocity of a moving target can be estimated by measuring the time rate change of phase at the output of the correlator due to the interference of the signals scattered off the target, measured at the receivers as the target passes by the array. In these works, this frequency has been shown to be

$$f_s = \omega D_\lambda \cos\theta \tag{6}$$

for CW unmodulated transmit waveforms, where D_λ is the baseline distance in wavelengths and θ is the angle between the target and the broadside of the array. By defining the angular velocity of the target as $\omega = \frac{d\theta}{dt}$, it follows that $\theta = \omega t + \theta_0$ where θ_0 is assumed to be zero. Thus, the angular velocity can be directly obtained by taking the time derivative of the phase term in (6) and solving for ω. For small angles the cosine term can be neglected (angles less than $\pm 25^\circ$ will deviate less than 10% from the ideal value). The angular rate measurement is then shown to be

$$\omega = \frac{f_s \lambda}{D}. \tag{7}$$

Linear velocity tangential to the array can be determined simply by applying the relation $\omega = v/R$, where R can be found using (5).

The angular velocity of a target can be obtained using an LFM signal in much the same way as typical Doppler processing of an LFM signal occurs, where the signal is sampled at the equiphase points on the waveform (i.e. the same location on the ramp), thus any variation in phase is due to a change in range of the target. In this way it acts as a CW signal being sampled at intervals of τ. In this case, because the frequency of the LFM ramp changes over time, the wavelength of the transmitted signal, and thus the spatial frequency of the fringe pattern, changes. Therefore, angular velocity measurements need to be taken at an equiphase point on the transmit waveform to ensure any shift in phase will be due to the angular velocity of the target as it passes through the fringe pattern of the array and not due to the changing spatial frequency of the fringe pattern.

C. Cross Range Angle Measurement

To measure the cross range angle, the forced frequency response of the grating lobes being swept across the target as the wavelength of the transmit waveform sweeps across the bandwidth of the chirp is exploited. This is performed using correlation of the signals received at each of the two receivers. Because the signal measured at the second receiver is a time-shifted copy of the signal measured at the first receiver, the correlation process is a function only of the geometric time delay (or advance), between the wavefront reaching first and second antennas, $\tau_g = \tau_{d2} - \tau_{d1} = \frac{D}{c}\sin\theta$, where θ is the angle of the target off broadside of the array and τ_{d1} and τ_{d2} are the round-trip time delays between the transmitter and receivers 1 and 2 respectively. The correlated signal is

$$\begin{aligned} r_c(\tau_g) &= r_1(t) r_2^*(t) \\ &= \exp\left\{ j\pi \left[2 f_0 \tau_g + \frac{\beta}{\tau}\left[\left(\tau_{d2}^2 - 2\tau_{d2} t\right) \right.\right.\right. \\ &\qquad \left.\left.\left. - \left(\tau_{d1}^2 - 2\tau_{d1} t\right) \right] \right] \right\} \\ &= \exp\left\{ j\pi \left[2 f_0 \tau_g + \frac{\beta}{\tau}\left(\tau_{d2}^2 - \tau_{d1}^2 - 2\tau_g t\right) \right] \right\}. \end{aligned} \tag{8}$$

Thus, because τ_d is dependent on R, for $v_R = 0$ the interferometric response can be shown to be

$$\begin{aligned} f_s(\theta) &= \frac{1}{2\pi}\frac{d\phi(t)}{dt} = -\frac{\beta}{\tau}\tau_g \\ &= -\frac{\beta}{\tau}\frac{D}{c}\sin\theta. \end{aligned} \tag{9}$$

From this, the angle of the target θ can be solved for directly as a function of the measured frequency at the output of the correlator

$$\theta = \sin^{-1}\left(-\frac{\tau}{\beta}\frac{c}{D} f_s \right). \tag{10}$$

Though a direct-downconversion was used in this derivation, the result is in agreement with the findings in [14].

For the dynamic case of (8), when $v_R \neq 0$, the frequency response can be found in a similar manner to the angular velocity measurement by letting $\theta = \omega t + \theta_0$ where ω is the cross range angular velocity of the target (θ_0 is assumed zero without loss of generality), then by taking the time derivative of the phase of (8) the frequency response is shown to be

$$\begin{aligned} f_s(\theta) &= \frac{1}{2\pi}\frac{d\phi(t)}{dt} \\ &= D_\lambda \omega \cos\theta + \frac{\beta}{\tau}\left[\frac{D}{c}\left(\sin\theta + \omega t \cos\theta\right) \right. \\ &\qquad \left. + \frac{4}{c^2}\left(R_2 v_{R2} - R_1 v_{R1}\right) \right] \end{aligned} \tag{11}$$

where R_n is the distance between the target and receiver n, and v_{Rn} is the radial component of the target velocity relative to receiver n. It can be seen that the angular velocity, as shown in (6), is present as the first term in this result. This implies that a coupling between the angle and angular velocity, similar to that found in range-Doppler coupling for range and radial velocity, is also found in angle measurements for dynamic targets when using an LFM waveform.

In practice, it may often be sufficient to estimate θ using the static case found in (9) even while targets are moving as the $\sin\theta$ term will typically dominate all others. This is due to the fact that when the target is moving only radially to the array (or is static) $v_{R1} \approx v_{R2}$ and $\omega = 0$. When the target has a component of angular velocity, the sum of the second term in the brackets is still insignificant compared to

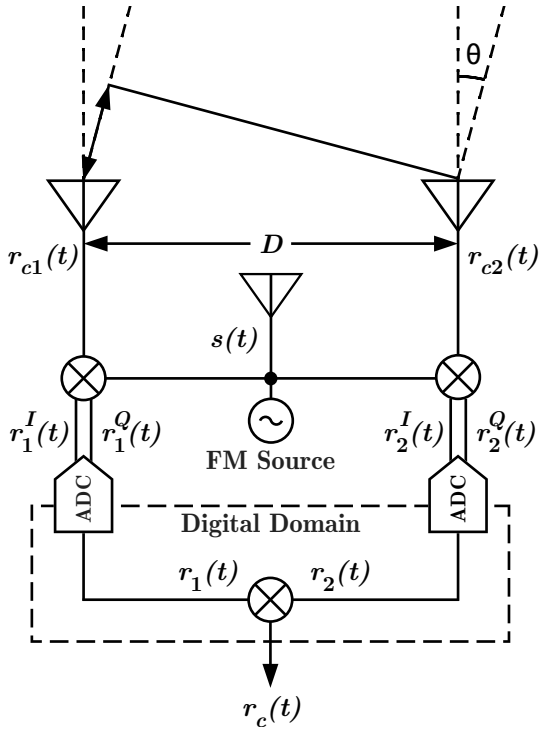

Fig. 2. Schematic of the proposed direct-downconversion digitally sampled radar.

the first, angular term. Furthermore, two assumptions must be made to use the static approximation: 1) $f_0 \gg \beta$ as is often the case for LFM systems, and 2) $\beta/\tau \gg f_0\omega$, i.e. the chirp rate is much greater than the product of the carrier frequency and the angular velocity of the target. The first assumption asserts that the angular velocity term will contribute significantly more to the approximation error than the $\omega t \cos\theta$ term. Thus, if assumption one is valid, error in the static approximation will be most noticeable as the target crosses broadside, where $\theta = 0$, as the only frequency shift will be due to the angular velocity component. However as the angle increases the frequency response of the angle will quickly dominate so long as assumption two is valid.

III. System Design

The design of an interferometric system to measure angle and angular rate will depend on the antenna baseline D, the wavelength λ, and the chirp-rate. For digital systems, the required sampling bandwidth is also a factor and will be discussed below.

A. Frequency Response Characteristics

Based on (9) it can be seen that the system response to the angle of the target is determined only by the antenna baseline D, and the chirp-rate β/τ while the response to the angular velocity is determined by the antenna baseline D, and the wavelength λ as shown in (6). Thus, it can be seen that for both measurements of angle and angular velocity that as the baseline increases, the frequency measured at the output of the correlator will also increase for the same measured quantity (angle or angular velocity). However, the chirp-rate and the wavelength can be used to control the desired frequency response for a measured angle and angular rate respectively, thus providing a mechanism to control each individually.

B. Sampling Criterion

When choosing a pulse repetition frequency (PRF), and a sampling rate for digitally sampled systems, as shown in Fig. 2, there may be varying criterion to consider to avoid aliasing. The maximum frequency of the interferometric angular measurement can be found from (9) by setting $\theta = \pm\pi/2$. The maximum frequency of the interferometric angular velocity measurement can be found using (6) and setting ω equal to the maximum desired angular velocity to be measured.

The sampling rate of the analog to digital converter (ADC) will be the Nyquist frequency of the larger of either the maximum interferometric angular measurement frequency, or the frequency which corresponds to the maximum range; this can be found using (5). Typically, this will be determined by the maximum range requirements. The PRF of the system will be determined by the Nyquist frequency of the larger of either the frequency corresponding to the maximum angular velocity measurement, or maximum Doppler shift required to be measured by the system.

It should be noted that because the correlation process only depends on the phase difference in the input signals, aliasing in the range-Doppler measurements sampled at the ADCs in Fig. 2 will not affect the angle and angular-rate measurements. Therefore, if range and Doppler measurements are not needed for a given application, sample-rate and PRF requirements may be relaxed in some cases.

IV. Simulation Results

The architecture simulated in this paper, seen in Fig. 2, consisted of a single transmitter capable of transmitting an FMCW waveform and two direct-downconversion receivers. All antennas were simulated using a raised cosine beam pattern approximation with a gain of 14 dBi. Each receiver was separated by a baseline D which was varied in length to illustrate its effect on the interferometric response. Following the down-converters the signal was sampled at $100\,\mathrm{kHz}$, then the discrete time samples were correlated.

Once the signals were correlated, the time series of complex measurements was arranged in an $N \times M$ matrix where N is the total number of pulses or "chirps", and M is the number of samples taken per chirp period T/τ where T is the sample period. An FFT was then applied row-wise (fast-time) to obtain the angle measurement and a second FFT was performed over the columns (slow-time) to obtain the angular velocity. For the angle FFT the window length was τ, the size was 2^{12}, and the overlap was 0%. For the angular velocity FFT the window length was $80\cdot\tau$, the size was 2^{17}, and the overlap was 95%. A Hamming window was used for both FFTs.

Four different simulations were run varying the pulse width τ, the antenna baseline D, and the center frequency f_0. For all

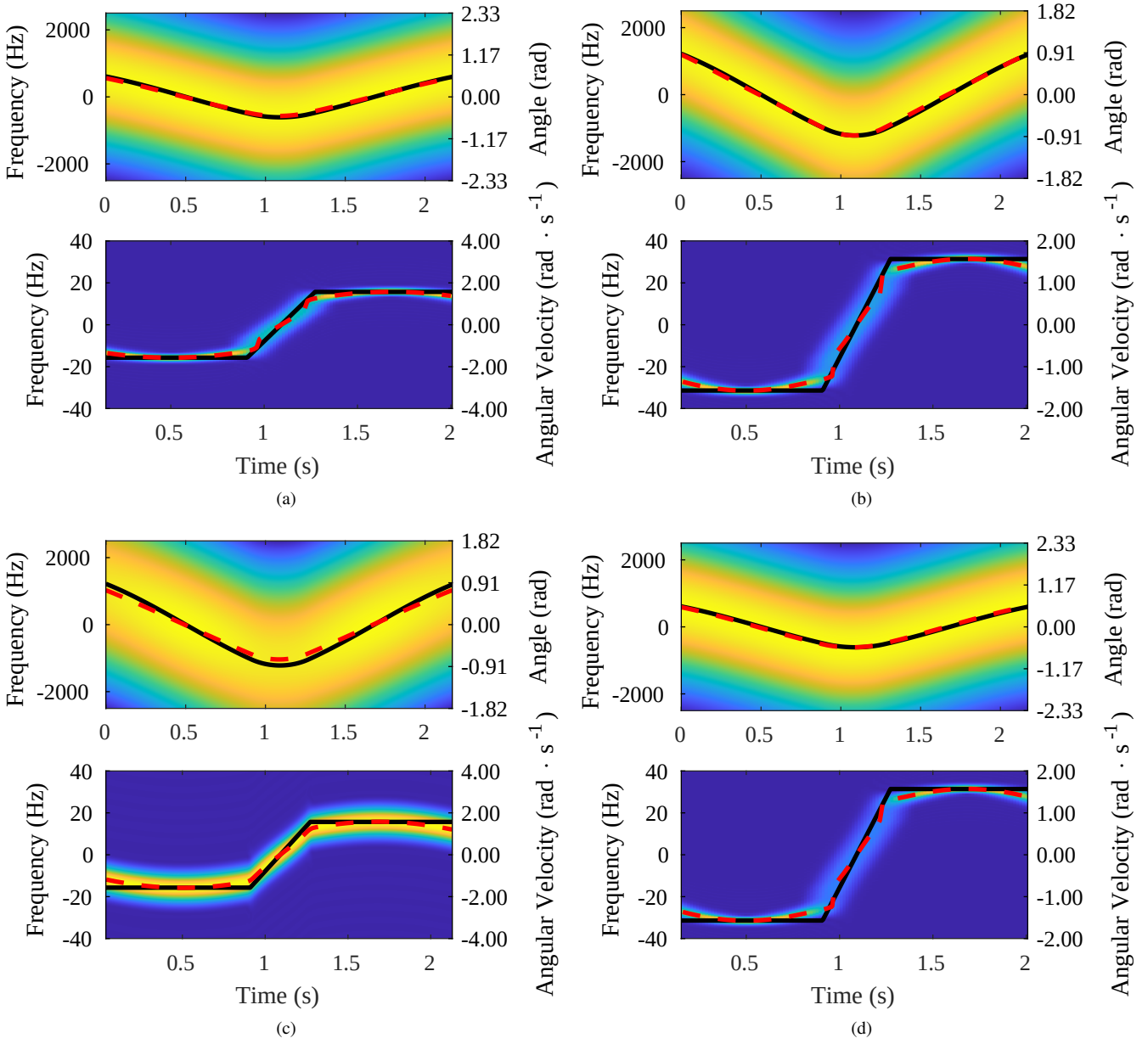

Fig. 3. The angle and angular velocity response at the output of the correlator for each simulation case. The estimates for each quantity (angle or angular velocity) are given by the red dashed line while the ground truth is in black. Note that due to differing window lengths used in the FFTs, the total length of the plots varies slightly. Simulation parameters: (a) $f_0 = 5.8\,\text{GHz}$, $\beta = 100\,\text{MHz}$, $\tau = 200\,\mu\text{s}$, $D = 10 \cdot \lambda$; (b) $f_0 = 5.8\,\text{GHz}$, $\beta = 100\,\text{MHz}$, $\tau = 200\,\mu\text{s}$, $D = 20 \cdot \lambda$; (c) $f_0 = 5.8\,\text{GHz}$, $\beta = 100\,\text{MHz}$, $\tau = 100\,\mu\text{s}$, $D = 10 \cdot \lambda$; (d) $f_0 = 11.6\,\text{GHz}$, $\beta = 100\,\text{MHz}$, $\tau = 100\,\mu\text{s}$, $D = 20 \cdot \lambda$.

simulations the trajectory, displayed as the solid black line in Figs. 3a–3d, consisted of a point-target starting at an angle of $\theta = \pi/4$ rad with a constant velocity of $\omega = -\pi/2$ rad·s^{-1}, moving to $\theta = -\pi/4$ rad where it decelerated at a rate of $\alpha = 5\pi/2$ rad·s^{-2}, then returned to $\theta = \pi/4$ rad ending with an angular velocity of $\omega = \pi/2$ rad·s^{-1}. The estimated values for θ and ω are shown as a red dashed line in Figs. 3a–3d where the estimate was computed by taking the frequency bin corresponding to the arg max of the power spectral density for each time in the plot.

For each of the simulations, values for f_0, β, τ, and D were chosen to be values that could be easily experimentally verified by existing systems. The baseline simulation is shown in Fig. 3a and used the parameters $f_0 = 5.8\,\text{GHz}$; $\beta = 100\,\text{MHz}$; $\tau = 200\,\mu\text{s}$ $D = 10 \cdot \lambda$. The baseline produced an angle estimate root-mean-square error (RMSE) of 0.0377 rad and an angular velocity estimate RMSE of 0.1784 rad·s^{-1}.

The second simulation, shown in Fig. 3b, increased the antenna baseline by a factor of two to $D = 20 \cdot \lambda$ while holding all other parameters constant. It can be seen that, as previously described, both the angle and angular velocity frequency responses have also been scaled by a factor of two.

This simulation produced an angle estimate RMSE of 0.0224 rad and an angular velocity estimate RMSE of 0.1613 rad·s^{-1}.

The third simulation, shown in Fig. 3c, decreased the pulse-width to $\tau = 100\,\mu s$ while holding all other parameters the same as the baseline simulation. As discussed in Section III-A, a variation in the chirp-rate will adjust the frequency response for the angular measurement while not effecting the angular velocity response. It is however important to note that the angular velocity sampling rate is determined by the PRF, thus varying τ for a CW radar will also have an effect on the Nyquist rate for the angular velocity measurement as discussed in Section III-B. The resulting simulation produced an angle estimate RMSE of 0.0767 rad and an angular velocity estimate RMSE of 0.176 rad·s^{-1}.

The fourth simulation, shown in Fig. 3d, doubled the chirp center frequency to $f_0 = 11.6\,\mathrm{GHz}$ while holding all other parameters the same as the baseline. It should be noted that D was held at the same distance in meters as the baseline but equates to $20 \cdot \lambda$ due to the change in carrier frequency. This illustrates that only the frequency response of the angular velocity measurement will increase while the angle measurement frequency response is held constant. This simulation produced an angle estimate RMSE of 0.0316 rad and an angular velocity estimate RMSE of 0.155 rad·s^{-1}.

V. Conclusion

This work has demonstrated the feasibility of a system which can simultaneously measure both the angle and angular velocity of a moving point-target. A simple relation between direct frequency measurement and the angle and angular velocity of the target have been derived and a technique for recovering each has been demonstrated. Simulated test cases have shown the systematic error in the measurements to be low, obtaining an angle RMSE of as low as 0.0224 rad and an angular velocity RMSE or as low as 0.155 rad·s^{-1}. This work demonstrates the viability of the interferometric radar for the simultaneous measurement the instantaneous angle and angular velocity of a moving point-target.

References

[1] M. A. Richards, *Fundamentals of Radar Signal Processing*, 2nd ed. New York, NY, USA: McGraw-Hill Education, 2014.

[2] M. Skolnik, *Introduction to Radar Systems*, 3rd ed. New York, NY, USA: McGraw-Hill, 2001.

[3] S. S. Blackman, *Multiple-Target Tracking with Radar Applications*. Norwood, MA, USA: Artech House, 1986.

[4] P. Bogler, *Radar Principles with Applications to Tracking Systems*. Wiley, 1990.

[5] X. R. Li and Y. Bar-Shalom, "Design of an interacting multiple model algorithm for air traffic control tracking," *IEEE Transactions on Control Systems Technology*, vol. 1, no. 3, pp. 186–194, 1993.

[6] D. Mehrholz, "Space object observation with radar," *Advances in Space Research*, vol. 13, no. 8, pp. 33 – 42, 1993.

[7] F. Folster and H. Rohling, "Data association and tracking for automotive radar networks," *IEEE Transactions on Intelligent Transportation Systems*, vol. 6, no. 4, pp. 370–377, 2005.

[8] Z. Zhang, Z. Tian, and M. Zhou, "Latern: Dynamic continuous hand gesture recognition using fmcw radar sensor," *IEEE Sensors Journal*, vol. 18, no. 8, pp. 3278–3289, 2018.

[9] V. C. Chen, F. Li, S.-S. Ho, and H. Wechsler, "Micro-doppler effect in radar: phenomenon, model, and simulation study," *IEEE Transactions on Aerospace and electronic systems*, vol. 42, no. 1, pp. 2–21, 2006.

[10] Y. Kim and T. Moon, "Human detection and activity classification based on micro-doppler signatures using deep convolutional neural networks," *IEEE Geoscience and Remote Sensing Letters*, vol. 13, no. 1, pp. 8–12, Jan 2016.

[11] X. Wang, P. Wang, X. Cao, and V. C. Chen, "Interferometric angular velocity measurement of rotating blades: theoretical analysis, modeling and simulation study," *IET Radar, Sonar Navigation*, vol. 13, no. 3, pp. 438–444, 2019.

[12] J. A. Nanzer and K. S. Zilevu, "Dual interferometric-doppler measurements of the radial and angular velocity of humans," *IEEE Transactions on Antennas and Propagation*, vol. 62, no. 3, pp. 1513–1517, March 2014.

[13] J. A. Nanzer, "Millimeter-wave interferometric angular velocity detection," *IEEE Transactions on Microwave Theory and Techniques*, vol. 58, no. 12, pp. 4128–4136, Dec 2010.

[14] S. Vakalis, E. Klinefelter, and J. A. Nanzer, "Angle estimation using wideband frequency modulation and an active distributed array," *IEEE Microwave and Wireless Components Letters*, vol. 28, no. 11, pp. 1059–1061, 2018.

[15] E. Klinefelter and J. A. Nanzer, "Radar measurement of the angular velocity of moving objects," pp. 219–243, 2019. [Online]. Available: https://digital-library.theiet.org/content/books/10.1049/pbce125e_ch9